Adaptive Control of Photolithography

Oscar D. Crisalle, Robert A. Soper, Duncan A. Mellichamp, and Dale E. Seborg
Dept. of Chemical and Nuclear Engineering, University of California, Santa Barbara, CA 93106

Adaptive control techniques, with their capability for providing satisfactory control even when the process changes with time, are promising candidates for dealing with common problems encountered in photolithography processing such as batch-to-batch variations in resist properties and inconsistencies in resist curing. In this article, an adaptive control strategy for the photolithography process is proposed and evaluated. The design utilizes a reduced-order lithography model, an on-line parameter estimator, and a nonlinear model-inversion controller.

The width of the printed resist lines, a crucial output of photolithography, is controlled by automatically adjusting the exposure energy. In the calculation of the appropriate exposure adjustment, the controller uses both measured critical-dimensions as well as estimated values produced by the process model. The control system is capable of tracking changes in the photolithography process by automatic updating of key model parameters as the process evolves in time. Simulation studies of the closed-loop adaptive control strategy, using the PROLITH simulation package to represent the lithography process, demonstrate the feasibility of this approach.

Introduction

The microelectronics industry continually moves toward the generation of smaller device and feature sizes, while simultaneously manufacturing integrated circuits on wafers of larger diameters. These trends require more effective process control strategies to prevent severe reductions in product yield and increases in operating costs (Fair, 1990; Jensen, 1986). Driven by progressively more demanding specifications, the crucial process of photolithography is required to deliver photoengraved lines and spaces of ever-decreasing widths. Even in the currently mature 1-μm technology, linewidth specifications are not always met with the desired consistency. The impact of photolithography performance on the successful manufacture of forthcoming submicron technology will be crucial. Improved control of photolithography is perhaps the most critical factor in realizing better manufacturing yields in the fabrication of integrated circuits with components of submicron dimensions.

The prototypical lithography process, shown in Figure 1, consists of six basic operations: substrate priming, photoresist spin-coating, pre-exposure bake, photoexposure, post-exposure bake, and film development. The problem of controlling photolithography is challenging, because the process involves a very large number of relevant variables that interact in complex ways. Particularly detrimental to process control activities is the fact that it is difficult to measure on-line many important variables (for example, the concentration distribution of photoactive component) or to quantify their effect on the process outputs (such as linewidth). A particularly relevant property of photolithography is that key process materials, as well as equipment and processing environments, experience time-varying fluctuations. Examples are the moisture content of photoresist films and the thickness of resist dry-skin produced during baking, neither of which can be easily measured by nondestructive methods on production wafers. Other typically unmeasured or unmeasurable time-varying disturbances include batch-to-batch inconsistencies in photoresist properties (viscosity, density, degree of polymerization, degradation of photoactive component, and so on), as well as inconsistencies in processing conditions (such as drifts in baking or development temperatures, changes in developer concentration, and pressure fluctuations in processing chambers).

The overall objective of a photolithography control program is to ensure that the outputs of the development step—the printed linewidth (often referred to as the *critical dimension* of the process), sidewall angle, registration, and step coverage—conform to established specifications. This objective is realized by adjusting one or several manipulated inputs and,

Correspondence concerning this article should be addressed to D. E. Seborg.
O. D. Crisalle is presently at the Department of Chemical Engineering, University of Florida, Gainesville, FL 32611.

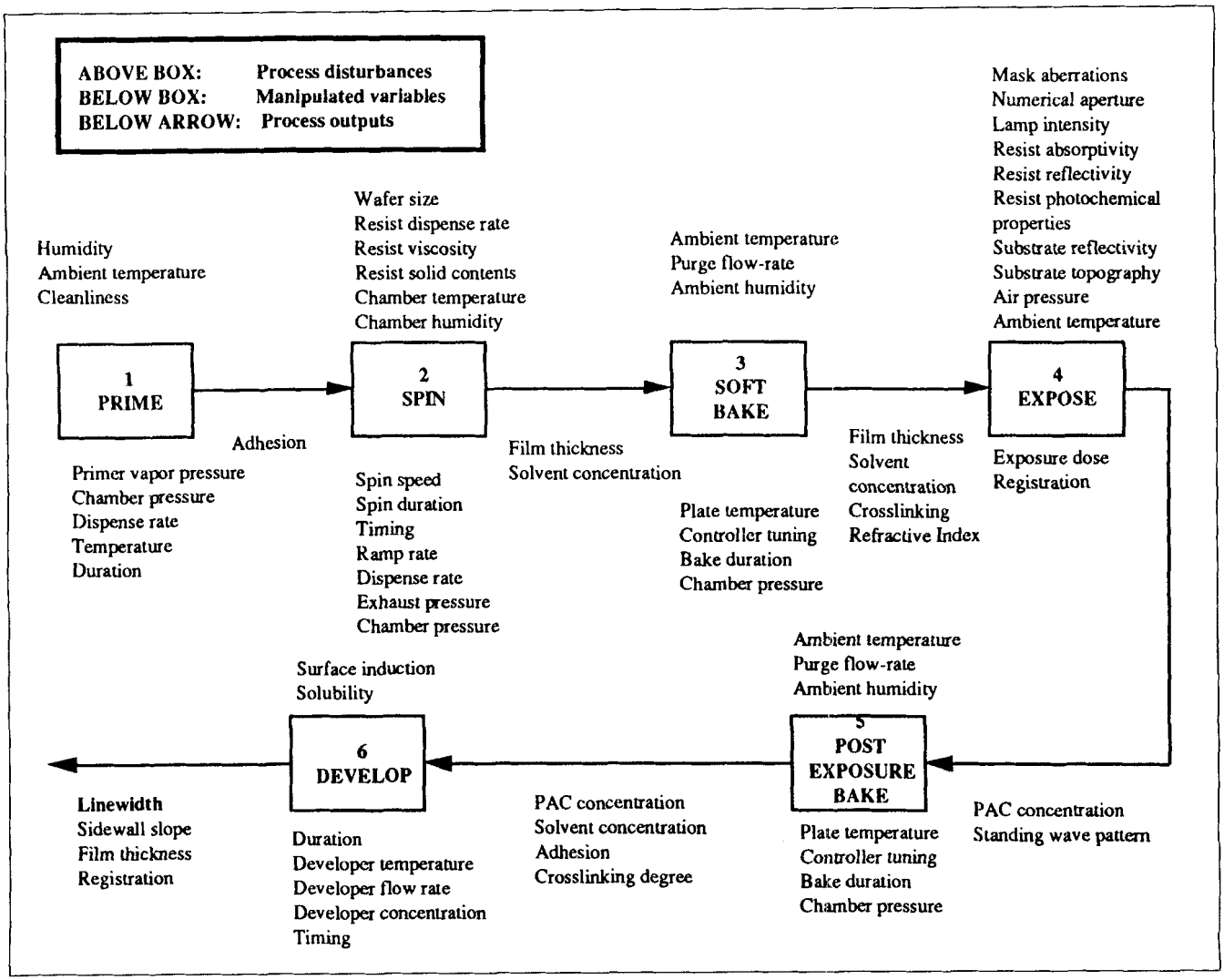

Figure 1. Photolithography process in block diagram form.

if possible, eliminating undesirable process disturbances that can be detected. Although all the process outputs are important, the critical dimension (CD) measure has traditionally been the most crucial. The CD is defined as the width of a photoresist line (or space) printed on a test pattern, specifically designed for characterizing the performance of the lithographic process.

Due primarily to the complicated nature of photolithography processing, no comprehensive control strategy exists yet. An important contribution to the current control technology, however, has been made by the use of statistical process control (SPC) methodology. This technique is also referred to as statistical quality control (SQC) and comprises two classes of activities: the routine use of process control charts and the regular implementation of statistically-based process characterization experiments. Control charts facilitate monitoring the time evolution of relevant variables, thus allowing the early detection of unfavorable process trends (Shewhart, 1986; Lorenzen and Vance, 1986; Chiu and Wetherill, 1974; Duncan, 1956, 1971). Characterization experiments, such as Hadamard-replicated experiments and surface-response analysis (Diamond, 1981), are used to quantify the effect of specific variables on the process outputs. The experiments can also suggest appropriate operating values (set points) for the manipulated variables.

When the SPC strategy is used, it is common practice to operate the lithographic process in an open-loop mode for relatively long periods of time, often four to six weeks. Control charting operations are routinely performed during this period. When the charts indicate the occurrence of a fault by the appearance of an abnormal output trend, the process is shut down, and the engineering staff intervenes to search for the cause of the fault. Processing resumes only when the fault causes are identified and eliminated.

Despite its widespread use in the microelectronics industry, SPC is not a panacea for every manufacturing control problem; the technique has several limitations. One shortcoming is that SPC does not provide sufficient assistance in identifying the causes of the manufacturing problem when the offending process variables are not routinely measured and therefore not charted. Also, a notable limitation of SPC is that, although the technology is capable of detecting abnormal process operation, it does not explicitly prescribe what corrective actions should be taken when assignable causes for the fault cannot be found. These shortcomings of SPC encumber the automatic

implementation of process adjustments and call for recurring intervention by engineering staff. Many of the limitations mentioned stem from the fact that fundamental understanding of photolithography is still incomplete; therefore, an open-loop control strategy such as SPC cannot effectively address all the process control problems of concern.

In the chemical industry, the classical method of controlling processes that are only partially understood is *closed-loop control*, where input and output variables are linked through information *feedback*. By analogy, it is reasonable to consider the possibility of designing and implementing a closed-loop control strategy that is particularly suited to the special characteristics of microelectronics processing and that would complement SPC by addressing its shortcomings. Adaptive control is a promising candidate. A primary reason for using adaptive control is that, being an automatic control method, it directly calculates the manipulation required to sustain adequate performance. This characteristic can reduce (or eliminate altogether) the need for engineering intervention. A second reason for using this technique is that the mechanism of adaptation can effectively counter the effect of the time-varying disturbances present in photolithography. Adaptive control, therefore, holds promise for promoting cost reduction by decreasing the amount of reworked or rejected material and diminishing the extent of required engineering involvement in day-to-day control operations. In addition, adaptive control would be a welcome element in process automation and CAM (computer-aided manufacturing) efforts in photolithography, because the technique is designed to be implemented in real time, integrating process models with automatic decision-making and on-line metrology.

Although it has already been argued that feedback control is an important strategy for successful photolithography manufacturing (Levy, 1984), the subject has not received very much attention in industry or academia. Notable exceptions are the work of Lauchlan et al. (1985) and of Ramirez and Carroll (1990) who have designed feedback systems for controlling the development operation. In addition, a simple integral-only controller for exposure dose adjustment is described by Hoerger (1988) and Hoerger et al. (1989). Crisalle (1990) discusses in detail the dynamic behavior of the photolithographic process and proposes a supervisory control framework which includes adaptive strategies. Although the application of adaptive control techniques to photolithography processing is not widespread, the idea of adaptation is nevertheless already recognized as a desirable feature in microelectronics manufacturing control. For example, a simple type of adaptive capability is displayed by projection steppers that measure the local temperature and barometric pressure to make focus corrections (Nagaswami, 1989).

This article describes the development and evaluation of a complete design for an adaptive control technique for photolithography processing. The control structure consists of a nonlinear controller and a reduced-order model containing only three parameters that can be updated on-line to track process changes. By automatic manipulation of the exposure energy, the critical dimensions are driven toward the specific target values whenever disturbances upset the photolithography process. Closed-loop simulations of the performance of the adaptive controller are used to evaluate the effectiveness of the control technique.

Methodology of Adaptive Control

The term adaptive control denotes a class of control strategies that update the parameters of a process model in real time. When the update or adaptation mechanism maintains a reasonably accurate process model at all times, the controller is capable of tracking process changes, thus allowing continued effective control even when the process undergoes structural changes or is affected by external perturbations. Adaptive control is particularly useful when incomplete fundamental process knowledge is available and when the process variables experience transient fluctuations. The utility of adaptive control has been demonstrated by numerous successful applications in the chemical, petroleum, and pulp and paper industries, where significantly improved control has been documented despite the complicated and time-varying nature of the underlying processes (Seborg et al., 1986).

An adaptive control strategy consists of three basic elements: (i) a process model, (ii) a parameter estimator, and (iii) a feedback controller. The process model is a relationship among the process input and output variables of interest. When the predicted output value is inaccurate, the model is deemed invalid and the model parameters are updated to better reflect the behavior of the process. The parameter adjustment operation is carried out by the parameter estimator, the second element in the adaptive structure. The third element, the feedback controller, calculates the appropriate value of the manipulated variable based on the current model parameters.

A number of alternative design strategies for adaptive control systems can be devised based on different choices for the three basic components discussed (Seborg et al., 1986). Notably, the design details for each of the basic elements depend strongly on the process to be controlled. Therefore, an adaptive control structure specifically suited for the characteristics of photolithography must be investigated. The next sections present explicit realizations of a lithography model, a parameter estimator, and a controller integrated into an adaptive control structure.

Reduced-Order Photolithography Model for Controller Design

Complete fundamental knowledge of the physical relation among the photolithography variables is not yet available. There do exist photolithography models that attempt to cope with the multidimensional nature of the process, such as those implemented in the programs SAMPLE (Oldham et al., 1979), PROLITH (Mack, 1985), PROSIM (Garza and Grindle, 1986), and SPESA (Bernard, 1985). Although these models provide quantitative process descriptions useful for the purpose of comparing alternative processing procedures and for analyzing process trends, they are too extensive for on-line production control. For the specific problem of synthesizing an adaptive controller for photolithography, it is desirable to base the design on a reduced-order model to avoid the very large dimensionality that results when all of the photolithography process variables are taken into account.

A reduced-order model facilitates the execution of all control tasks by significantly simplifying the control calculations. It also alleviates the load on the parameter estimator, because fewer input/output signals and parameters are involved. For example, a simple lithography model could consist of a single

equation containing only a small number of parameters and relating one input, the exposure energy, to one output, the resulting critical dimension. A photolithography model with these characteristics, called the Hershel-Mack lumped-parameter model, has been reported (Mack et al., 1987; Hershel and Mack, 1987).

The lumped-parameter model (LPM) of Hershel and Mack provides an explicit relationship between the critical dimension (a controlled variable) of the line or space feature, and the exposure energy (a manipulated input variable) by means of the integral equation:

$$\left[\frac{E}{E_o}\right]^{\gamma_e} = 1 + \frac{1}{D_e}\int_0^x \left[\frac{I(\xi)}{I(0)}\right]^{-\gamma_e} d\xi \qquad (1a)$$

where

x = $CD/2$ if the feature is a space
x = $(P-CD)/2$ if the feature is a line
CD = critical dimension
P = photomask pitch
E = exposure energy
E_o = effective photosensitivity
D_e = effective film thickness
γ_e = effective resist contrast
$I(\xi)$ = aerial intensity distribution
ξ = horizontal location on the mask

Equation 1a is valid only for exposure energies satisfying $E > E_o$. For the case $E \le E_o$, the model reduces to:

$$CD = \begin{cases} 0 & \text{if the feature is a space} \\ P & \text{if the feature is a line} \end{cases} \qquad (1b)$$

The model in Eq. 1a is a single-input/single-output relationship that includes the combined effects of the exposure and development operations. The model contains three empirical parameters, E_o, D_e, and γ_e, and requires knowledge of the aerial intensity distribution function $I(\xi)$.

Because the three LPM parameters are empirical and lump together a large number of complicated effects, one should be cautious about assigning fundamental physical meanings to them. However, the effective photosensitivity E_o can be regarded as the lowest bound on the energy needed to allow complete dissolution of the resist film in a given development time. This view is supported by considering that exposure with an energy equal to E_o requires that the upper integration limit in Eq. 1a be identically zero for the equality to hold (a zero-width space). This is the limiting case where the development process fails to open a space through the film. Consequently, an exposure energy greater than E_o is necessary to produce a well-defined line/space pattern in the film. Therefore, from this perspective E_o is a threshold energy value, and as such it is expected to be a strong function of the duration of the development step.

The aerial intensity distribution $I(\xi)$ appearing in the integrand of the LPM equation represents the energy dose delivered by the exposure tool along the horizontal direction ξ, where by convention, $\xi = 0$ corresponds to the center of the mask space. The intensity distribution produced by optical projection cameras currently in use in manufacturing facilities can be theoretically modeled as a partially coherent imaging problem (Subramanian, 1981; Yeung, 1988). Calculation of $I(\xi)$ can be carried out numerically using standard imaging routines

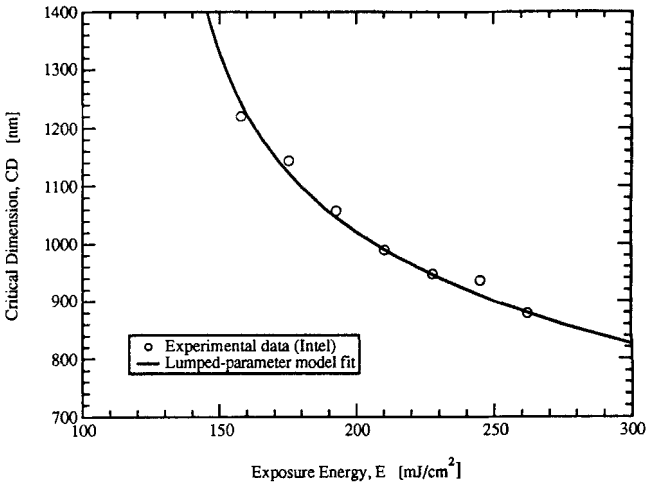

Figure 2. Lumped-parameter model fit to industrial data.

such as those found in SAMPLE and PROLITH. All that is required is knowledge of the optical properties of the imaging tool, namely, the illumination wavelength, degree of coherence, numerical aperture of the lens, shape of the pupil, and the amount of defocus. It is also possible to measure the intensity distribution on-line using technology that is commercially available (Norton and Cheng, 1988). The method consists of measuring the intensity of the light that is scattered from a specially calibrated wafer. This intensity measurement technology further strengthens the usefulness of the LPM model.

The LPM model has been shown to exhibit excellent agreement with experimental data. Hershel and Mack (1987) obtained good model-process agreement for linewidths greater than 1 μm. The model is also valid for submicron linewidths, as illustrated in Figure 2 where critical dimension data collected in a fabrication facility of the Intel Corporation in Santa Clara, California, are well fitted by the model. The data were produced using a 5X stepping projection aligner, with a narrow exposure band centered about a wavelength of 436 nm, a 0.35 numerical aperture, and an illumination coherence factor of 0.7. The film is 1,300 nm thick, and the development method consisted of a two-phase spray-puddle cycle of 29-second duration.

It must be noted that the *empirical* LPM parameters E_o, D_e, and γ_e are not necessarily equal to the *actual* process parameters E_o' (photosensitivity), D' (film thickness), and γ' (contrast), which are commonly used to characterize the photolithography process (Thompson et al., 1983). The reason for this disagreement is that the LPM parameters lump together multiple exposure and development effects to make possible a single-equation representation of the process. The LPM parameters used for the fit in Figure 2 are $D_e = 1{,}281$ nm, $\gamma_e = 3.1$, and $E_O = 118$ mJ/cm^2, whereas the actual experimental parameters are $D' = 1{,}300$ nm, $\gamma' = 1$, and $E_O' = 122$ mJ/cm^2. The LPM parameters were found by a simple trial-and-error procedure and inspection of the resulting fit.

The three-parameter LPM equation is an excellent candidate model to use in developing model-based and adaptive control strategies for photolithography. A significant advantage of the model is that it brings about great simplification in the description of the photolithography process, because it consists of a single equation. The model usefulness is validated by the

fact that it is capable of representing experimental critical dimension data at the submicron level.

Parameter Estimation

The task of the parameter estimator is to produce numerical estimates of E_o, D_e, and γ_e such that for a given exposure energy E, the LPM equation (Eq. 1) yields an estimated critical dimension value $\widehat{CD}$ that is close to the experimentally observed CD. In this section, we develop a general methodology for calculating the LPM parameters from experimental photolithography process data. The data required for estimating the parameters are experimental critical dimension measurements for various exposure energies, such as the data shown in Figure 2. All three parameters can, in principle, be fit to the data using the least-squares method.

Generation of data for parameter estimation

The estimation data are obtained by periodic sampling of the process variables. Critical dimension measurements taken at a given instant t are denoted as $CD(t)$. The measurement $CD(t)$ may represent the average critical dimension for a single wafer or for a batch of wafers (a group of 50 wafers traveling through the process in the same container), or the average CD for a process lot (a group of wafer batches). The frequency of sampling (whether measurements are taken for every wafer, every batch, or every lot) depends on the resources available for sampling, such as the number of available scanning electron microscopes, throughput considerations, and economic constraints. In practice, appropriate sampling frequencies are selected after careful consideration of all these issues.

The following discussion uses the convention that subscripted measurements, such as $CD_1(t)$ and $CD_2(t)$, represent measurements taken at the same sampling instant but made at wafer locations that have been exposed using different doses. For example, $CD_1(t)$ may represent the average CD measured at a test pattern exposed with a dose of, say, 150 mJ/cm^2, whereas $CD_2(t)$ would represent a measurement at a test pattern exposed at a different dose, say, 250 mJ/cm^2.

The data for parameter estimation can be generated using a simple experiment. At a given instant t, N test patterns (or N wafers) are exposed using different input doses $E_1, E_2, \ldots, E_N$, and a corresponding N-tuple of output measurements $CD_1, CD_2, \ldots, CD_N$ is obtained. The number of measurements N must at least be equal to the number of parameters to be identified. Figure 3 shows a block diagram for the data-generation operation for the special case where $N = 3$. The figure also shows the linkage between the data and the on-line parameter estimator responsible for producing the estimated LPM parameters.

Least-squares estimation of parameters D_e, γ_e, and E_O

A nonlinear parameter fitting procedure is used to calculate values for the LPM parameters D_e, γ_e, and E_O which minimize a least-squares criterion. In this approach, the LPM parameters are calculated using the N-tuple of CD measurements taken at the current instant t (a discrete value representing the sample number), as well as previous N-tuples obtained at previous instants t-1, t-2, etc., which are all incorporated in the quadratic least-squares criterion:

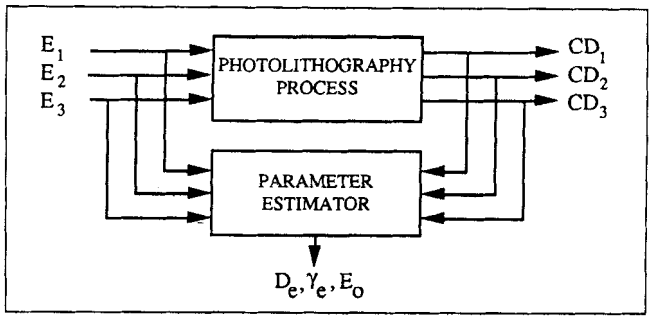

Figure 3. Photolithography parameter estimator.

$$J(t) = \sum_{j=t-j^*}^{t} \lambda^{t-j} \sum_{i=1}^{N} \epsilon_i(j)^2 \tag{2}$$

where the residual $\epsilon_i(t)$ is defined as:

$$\epsilon_i(t) = CD_i(t) - \widehat{CD}_i(t) \tag{3}$$

and $CD_i(t)$ is the critical dimension measured at sampling instant t and produced with exposure energy $E_i(t-1)$; $\widehat{CD}_i(t)$ is the estimated critical dimension using the LPM model; N is the number of exposure energy inputs used at time t; λ is the forgetting factor ($0<\lambda\leq 1$); and j^* is the forgetting horizon ($0\leq j^*\leq t$).

Finding the LPM parameters which minimize Eq. 2 is a nonlinear least-squares estimation problem that can be solved using a number of alternative procedures, including the Levenberg-Marquardt algorithm (Dennis and Schnabel, 1983; Edgar and Himmelblau, 1988) which is employed in this investigation.

The on-line estimation method incorporates the capability of forgetting old data to allow tracking the model parameters when the process experiences changes caused by equipment or material aging or by unmeasured disturbances (Ljung, 1987). Forgetting is achieved by weighting each N-tuple with powers of the forgetting factor λ. Recent N-tuples are weighted more heavily than older N-tuples. The forgetting horizon index j^* in Eq. 2 is used to specify the number of past N-tuples that are included in the estimation process. The forgetting horizon can be deliberately set equal to zero when resetting or reinitialization of the estimation procedure is desired. When $j^*=0$, only the most recent N-tuple of data is used.

Ideally, the N exposure energies E_i should be equally distributed within an operating window and centered about a nominal exposure energy. The width of the energy window is a parameter that must be specified by the user. A small value of N allows the estimation experiment to be conducted using the test patterns of a regular production wafer, thus avoiding the necessity of performing a specialized experiment on dedicated wafers. As the results in the Simulation Study section show, a value of $N=3$ is adequate when all three LPM parameters are estimated.

The number of CD measurements required for parameter estimation is a significant issue, because submicron resist features can only be measured using a scanning electron microscope (SEM) which has low throughput. Thus, dedicating equipment time to the measurement of control-related CD's, rather than supporting the measurement of final-product linewidth, may be costly. Minimization of SEM load is impor-

tant to the commercial success of the manufacturing operation and must be recognized as an important objective in the control strategy.

Filtering critical dimension data used for parameter estimation

The measured critical dimension values used in the calculation of the residuals of Eq. 3 can be filtered to prevent parameter drift caused by measurement noise. For example, the following first-order filter effectively attenuates the contribution of high-frequency noise to the measurements:

$$CD_i'(t) = \alpha_e CD_i'(t-1) + (1-\alpha_e) CD_i(t), \; i = 1,2, \ldots, N \quad (4)$$

where $CD_i(t)$ is the raw measurement at sampling instant t; $CD_i'(t)$ is the filtered measurement; and α_e is the estimation filter constant ($0 \le \alpha_e < 1$). Filtering begins with the initial condition, $CD_i'(0) = CD_i(0)$.

The filtered value $CD_i'(t)$ is used instead of the actual measured value $CD_i(t)$ in Eq. 3. Note that when $\alpha_e = 0$, no filtering occurs and the raw measurement is used. At the other extreme, heavy filtering occurs as α_e approaches 1. The recommended values of α_e for this application are in the range between 0.3 (mild filtering) and 0.6 (heavy filtering).

Nonlinear Model-Inversion Controller

The feedback controller is responsible for adjusting the exposure energy to maintain adequate critical dimension control at all times. A new model-based control strategy based on the following nonlinear control law is proposed in this research:

$$E(t) = E_o \left\{ 1 + \frac{1}{D_e} \int_0^{x_1(t)} \left[\frac{I(\xi)}{I(O)} \right]^{-\gamma_e} d\xi \right\}^{\frac{1}{\gamma_e}} \quad (5)$$

where

$$x_1(t) = \frac{CD^s + \widehat{CD}(t) - CD(t)}{2}$$

if the feature is a space, or

$$x_1(t) = \frac{P - CD^s - \widehat{CD}(t) + CD(t)}{2}$$

if the feature is a line. The estimated critical dimension $\widehat{CD}(t)$ is calculated using the three model parameters D_e, γ_e, and E_o in the LPM equation:

$$\left[\frac{E(t-1)}{E_o} \right]^{\gamma_e} = 1 + \frac{1}{D_e} \int_0^{x_2(t)} \left[\frac{I(\xi)}{I(O)} \right]^{-\gamma_e} d\xi \quad (6)$$

with

$$x_2(t) = \frac{\widehat{CD}(t)}{2}$$

if the feature is a space, or

$$x_2(t) = \frac{P - \widehat{CD}(t)}{2}$$

if the feature is a line and where $E(t-1)$ is the energy used to produce the measured critical dimension $CD(t)$.

This *nonlinear model-inversion controller* (NMIC) is completely defined by Eqs. 5 and 6. Equation 5 corresponds to an inversion of the LPM model, since it expresses the manipulated input (exposure energy) as a function of a process output (critical dimension). This equation can be solved in a straightforward manner by numerical integration of the right side of Eq. 5. But, before Eq. 5 can be implemented, Eq. 6 must be solved for $\widehat{CD}(t)$. Because the latter equation is implicit in its output, solving for $\widehat{CD}(t)$ requires the use of a numerical root-finding procedure.

A parameter estimator is used to allow the NMIC controller to operate in an adaptive mode. The relationship among the controller, the LPM lithography model, and the parameter estimator is represented in Figure 4. The parameter estimation block produces estimates of the process parameters D_e, γ_e, and E_o, which are made available to the controller and to the process model. The controller block calculates the manipulation E according to Eq. 5, and the LPM process model block calculates $\widehat{CD}$ according to Eq. 6.

The proposed NMIC structure features a parallel arrangement of the model and the process. Such a configuration has been derived for linear systems by Youla et al. (1976). Garcia and Morari (1982) made such a parallel configuration the central theme in the design of controllers for linear systems using the internal model control (IMC) principle (Seborg et al., 1989). Extensions to the nonlinear case have been reported by Economou et al. (1986) and Henson and Seborg (1991).

The NMIC design introduces several innovations. First, a controller that implements model inversion of a nonlinear process model has been successfully synthesized. Second, the controller design is based on a static model, rather than a dynamic model that would normally be utilized in the IMC methodology. Finally, the controller design has been integrated into an adaptive scheme with a nonlinear parameter estimator specifically tailored to the process of photolithography.

Filtering the CD measurement for the controller calculations

The CD measurement used in the feedback loop may be corrupted by noise introduced by measurement inaccuracies

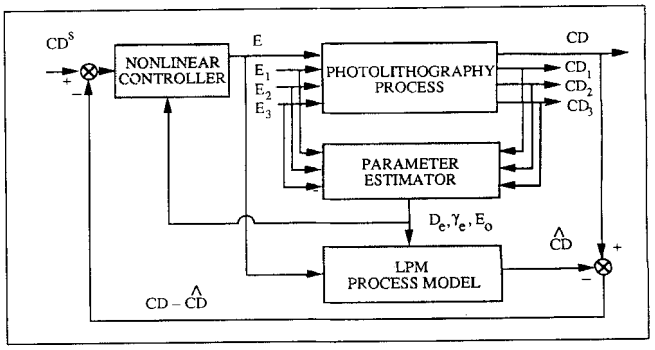

Figure 4. Proposed adaptive control strategy for photolithography based on nonlinear model inversion control and the LPM model.

or by stochastic disturbances. When the noise component of the measured signal is large, the controller makes inappropriate adjustments, because it responds to random fluctuations, rather than to actual process trends. This undesirable effect can be prevented by use of a filter that attenuates the noise contribution to the measured signal.

The desired noise attenuation effect is achieved by substituting the actual measurement $CD(t)$ in Eqs. 5 and 6 with a filtered version, $CD''(t)$. Filtering can be accomplished with a first-order filter with the same structure as that of Eq. 4:

$$CD''(t) = \alpha_c CD''(t-1) + (1-\alpha_c) CD(t) \tag{7}$$

where α_c is the control filter constant ($0 \le \alpha_c < 1$). The initial condition for the filter is $CD''(0) = CD(0)$. Suitable values for α_c lie in the range between 0.3 and 0.6.

Control filtering is an important operation for reducing the effects of stochastic disturbances in both adaptive and nonadaptive feedback control systems. In conjunction with the estimation filter (Eq. 4), the control filter can significantly improve the performance of the control loop. It is natural to set $\alpha_c = \alpha_e$; however, each filter constant can be independently specified because the estimation and feedback filters have different functions. The estimation filter is responsible for reducing the corrupting effect of noise on the parameter estimates, whereas the control filter is designed to prevent the controller from making noise-induced random adjustments.

Control deadband

Because commercial projection step-and-repeat steppers have a bound on the fastest reproducible shutter speed (typically, about 3 ms), smaller exposure time adjustments are not possible. This limitation on the control action is expressed in terms of a deadband variable, $\Delta E_{\min}$, the minimum allowable exposure energy change. No attempt is made to adjust the exposure dose when this threshold is not exceeded. The control policy can then be expressed by the logical condition:

$$\text{If } \left| E(t) - E(t-1) \right| \le \Delta E_{\min}, \text{ then } E(t) = E(t-1) \tag{8}$$

The control deadband $\Delta E_{\min}$ may be arbitrarily set to values greater than the resolution of the optical shutter. Such a choice prevents the controller from making small exposure adjustments that would have only a minor effect on the critical dimensions. The performance of the control loop is thus markedly enhanced.

Simulation Study

A successful photolithography controller must be able to perform well over a wide range of process conditions and must also be capable of rejecting the effect of unknown disturbances on the critical dimension. The performance of the proposed control strategy can be evaluated effectively using a process simulator that can emulate a production environment. Control system performance is typically evaluated using set-point change tests and disturbance rejection tests. Large set-point changes were specified to force the controller to operate over a wide range of exposures. In the disturbance-rejection tests, the controller was required to cope with process disturbances of unknown (or unmeasured) origin. Three disturbances that can occur in practice were considered: (i) changes in photoresist thickness, (ii) changes in the degree of defocus, and (iii) changes in photoresist absorptivity.

The process equipment simulated is representative of a typical high-resolution, single-track lithography line that comprises a resist coating unit (spinner), a pre-exposure bake oven, a projection step-and-repeat camera, a post-exposure bake oven, and a single-wafer immersion development station. Relevant characteristics of the resist and optical systems used are summarized in Table 1. The printed line *CD* was measured using the band method, which has been shown to provide a good characterization of the linewidth near the bottom of the feature (Crisalle et al., 1989). Additional details concerning the simulation study are available elsewhere (Crisalle, 1990).

The photolithography process was simulated using the PROLITH program (Mack, 1985) and a customized FORTRAN driver loop that coordinates the action of a parameter estimation routine and a controller routine. The parameter estimation problem is solved numerically using the Moré implementation of the Levenberg-Marquardt algorithm in the MINPACK library of FORTRAN subroutines (Moré et al., 1980) based on analytical expressions for the Jacobian of the residual vector rather than finite-difference approximations. At every sampling instant, the parameter estimation calculations are performed using three *CD* measurements ($N=3$) corresponding to the energy doses: $E_1 = 115$ mJ/cm^2, $E_2 = 140$ mJ/cm^2, and $E_3 = 165$ mJ/cm^2.

The execution-time requirements of the program are considerable, because the simulator makes a very large number of subroutine calls to the PROLITH program (used at its highest accuracy level). This consideration led to choosing a Cray Y-MP supercomputer as the hardware platform. However, we wish to emphasize that such a high-performance computer is not required for implementation of the strategy in an industrial application because the control algorithms and the parameter estimation routines have only modest execution requirements: they can run in a typical engineering workstation or personal computer.

Set-point change test

Representative results for set-point changes are shown in Figure 5 where step changes in set point are made with the

Table 1. Resist and Optical System Used in the Simulations

Resist Type	Kodak 820	Wavelength [nm]	436
Thickness [nm]	1,300	Coherence Factor	0.70
Substrate	Silicon	Numerical Aperture	0.35
Development Time [s]	30	Mask Line Width [nm]	850
Bake Diffusion Length [nm]	54.1	Mask Pitch [nm]	1,700
Lamp Intensity [mW/cm^2]	100	Defocus [nm]	0

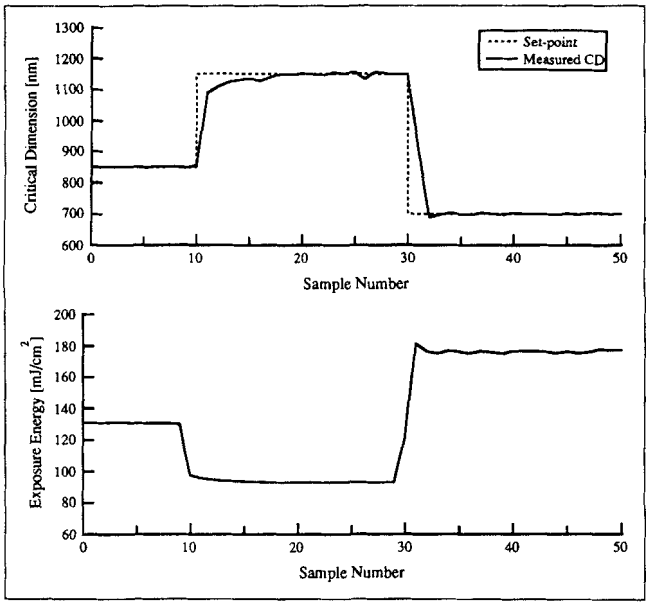

Figure 5. Response of a nonadaptive NMIC controller to a series of set-point changes.

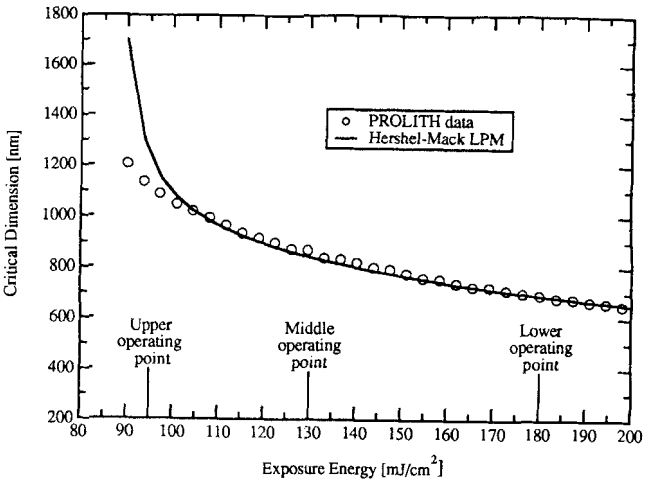

Figure 6. LPM fit to simulated data over a wide range of exposure energies.

controller adaptation mechanism turned off so that the LPM parameters are constant at all times. The following LPM parameters, determined by simple inspection of the fit to simulated CD data from PROLITH, were used: $D_e = 1{,}535$ nm, $\gamma_e = 4.9$, and $E_o = 90$ mJ/cm^2. The *CD* data were unfiltered ($\alpha_e = \alpha_c = 0$), and the controller was not constrained with a deadband ($\Delta E_{min} = 0$). For clarity, consecutive measurements of critical dimensions and exposure energy are joined with straight-line segments in the figure, although it is understood that the data represent a series of discrete measurements.

Figure 5 indicates that in the initial region of operation (set point equal to 850 nm) the controller successfully maintains the CD at this target value. When a change of set point occurs at the tenth sampling instant, the controller adjusts the exposure energy to drive the CD to the second region (set point equal to 1,150 nm). After another set-point change occurs at the 30th sampling instant, the controller aggressively changes the exposure energy and succeeds in rapidly bringing the process CD to the third operating region (set point equal to 700 nm). Note that while in the lowest operating region, the controller makes aggressive exposure adjustments to drive the critical dimension to the set point, at the highest operating point, the controller acts more cautiously and is more sluggish in reaching the set point. The sluggish behavior arises because the chosen LPM parameters define a model that fits the process behavior particularly well in the middle and lower operating regions, but has large errors in the high region, as indicated in Figure 6. Note that in spite of the process-model mismatch in the high set-point region, the controller is still quite successful, illustrating that the NMIC design has a built-in capability for coping with a reasonable amount of model uncertainty.

In these simulations, the *CD* does not always follow a smooth trajectory after the new set point is reached. Small deviations (of approximately 15 nm or less) from set point persist. The reason for this behavior is that measurement noise is introduced when one attempts to characterize a wavy resist sidewall (standing-wave effect) with a single critical dimension value (Crisalle et al., 1989). Measurement noise tends to corrupt *CD* measurements that are taken in a production environment, where a scanning electron microscope is used as the measurement tool. An undesirable effect of this low-level noise is that it prompts the controller to produce small exposure adjustments that are in fact unnecessary. Fortunately, this problem can be eliminated using the filter and the control deadband technique discussed earlier.

The set-point changes in Figure 5 show that the NMIC controller is capable of delivering high-performance control even when the underlying model does not describe the photolithography process with great accuracy. Further improvement in performance can be obtained at the higher set point by operating in an adaptive mode, because the estimator will provide a better model representation in this energy range.

Thickness disturbance

Resist thickness variations are common disturbances in a photolithography line and can cause large critical-dimension shifts in narrow bandwidth exposure systems (Bruce et al., 1989). In Figure 7 a nonadaptive NMIC controller with constant parameter values, $D_e = 1{,}535$ nm, $\gamma_e = 4.9$, and $E_o = 90$ mJ/cm^2, is used to control the *CD* when large thickness disturbances take place at sampling instants 10 and 40. No filters or control deadband are used.

Note that a *CD* deviation of approximately 130 nm appears when the first disturbance takes place at $t = 10$. The controller reacts by reducing the exposure energy and is successful in returning the critical dimension to the set point in a few steps. Analogous behavior is observed when the next step disturbance takes place at $t = 40$. In this simulation, the NMIC controller successfully copes with an important process disturbance, in a fully automated fashion that eliminates the need for engineering intervention. As discussed for the preceding set-point change test, the nonsmoothness of the *CD* trajectory is caused by measurement noise; and its effect on the feedback controller can be significantly reduced.

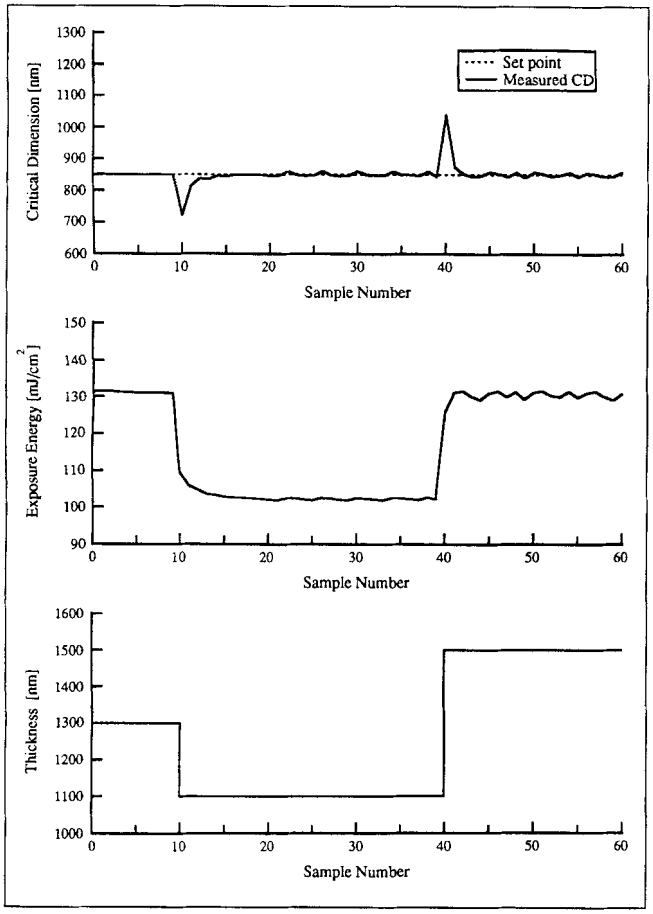

Figure 7. Thickness disturbance: closed-loop response of a nonadaptive NMIC controller.

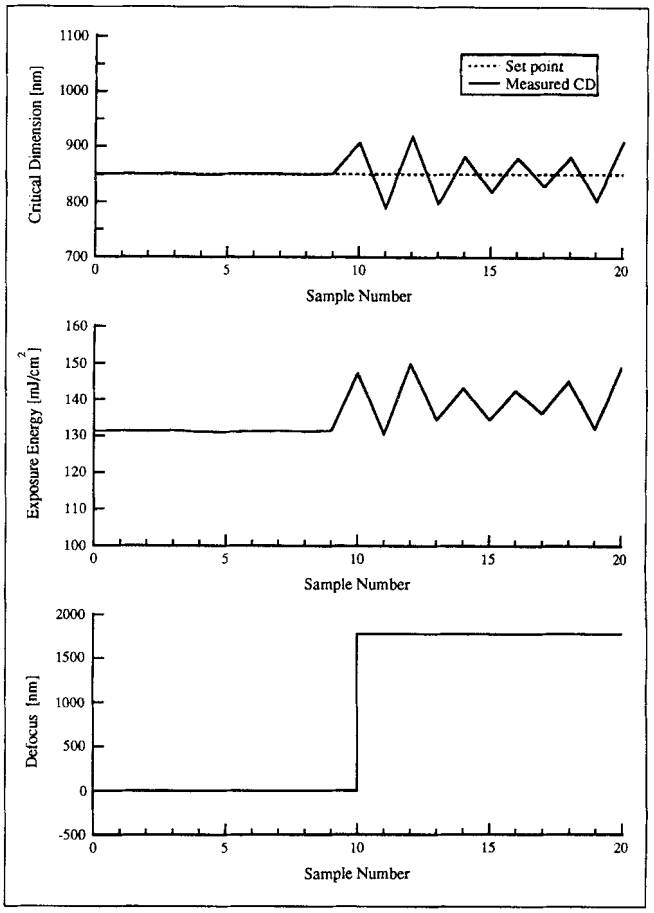

Figure 8. Defocus disturbance: closed-loop response of a nonadaptive NMIC controller.

Clearly, in an industrial photolithography line, the large process faults induced by such thickness disturbances would not have escaped detection by the engineering staff. Measures would have been taken to eradicate the problem, for example, by adjusting the resist coating equipment. Nevertheless, the disturbance rejection test dramatically demonstrates the powerful capabilities of the NMIC design. If the *CD* deviations observed in this simulation had been triggered by a disturbance that is not as easily detectable as a thickness change, then the NMIC strategy would still have returned the process to the set point, because the controller does not require any knowledge whatsoever about the sources or magnitudes of the disturbances.

Defocus disturbance

A defocus error in the exposure equipment is a process disturbance that is difficult to measure and therefore can easily remain undetected. To simulate the effect of this type of disturbance, a defocus error of 1 Rayleigh unit (1,779 nm) is introduced at $t = 10$ in Figure 8, while the process is in closed-loop mode using a nonadaptive NMIC controller ($D_e = 1{,}535$ nm, $\gamma_e = 4.9$, $E_o = 90$ mJ/cm^2, $\alpha_e = \alpha_c = 0$, and $\Delta E_{\min} = 0$). Good performance is observed only until the defocus error occurs, at which point the controller performance degrades; and it fails to bring the *CD* to set point and settles into an oscillating exposure-adjustment pattern. The reason for the poor controller performance is that the constant values of the LPM parameters available to the NMIC controller do not model the defocused process well; therefore, adaptation is required to improve performance.

One adaptation scheme that could be used is off-line adaptation. In this approach, when a large critical-dimension deviation is detected (using SPC monitoring techniques, for example) the engineering staff initiates a parameter estimation experiment with the intention of obtaining parameters that better describe the perturbed photolithography process. The NMIC controller then resumes operation using the new parameter values. In the simulation shown in Figure 9, the model parameters are initially fixed ($D_e = 81.3$ nm, $\gamma_e = 1.74$, and $E_o = 32.2$ mJ/cm^2). When the effect of the defocus perturbation causes a *CD* disturbance at $t = 10$, a new parameter estimation experiment is carried out and updated parameter values are obtained ($D_e = 607.3$ nm, $\gamma_e = 1.47$, and $E_o = 79.4$ mJ/cm^2). With the updated model, the NMIC controller is capable of making effective exposure-energy adjustments to drive the *CD* to the set point.

The adaptation scheme can also be performed on-line. In this case, the parameter estimation mechanism is active at every sampling instant and provides the NMIC controller with an updated set of parameters, which is used for the current exposure adjustment calculation. Figure 10 shows the *CD* trajectory obtained when an adaptive NMIC controller adjusts

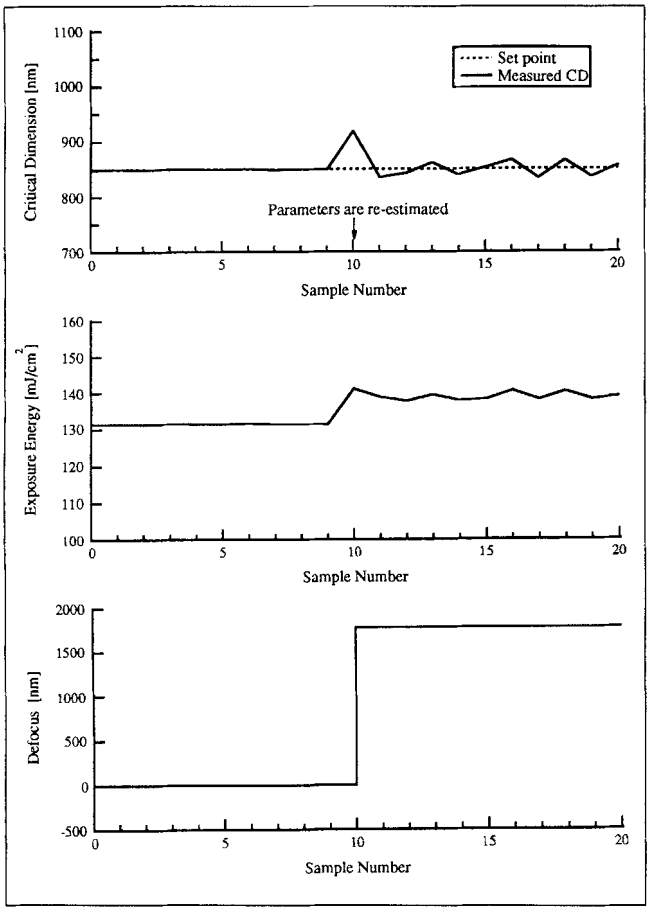

Figure 9. Defocus disturbance: closed-loop response of an adaptive NMIC controller with off-line parameter estimation.

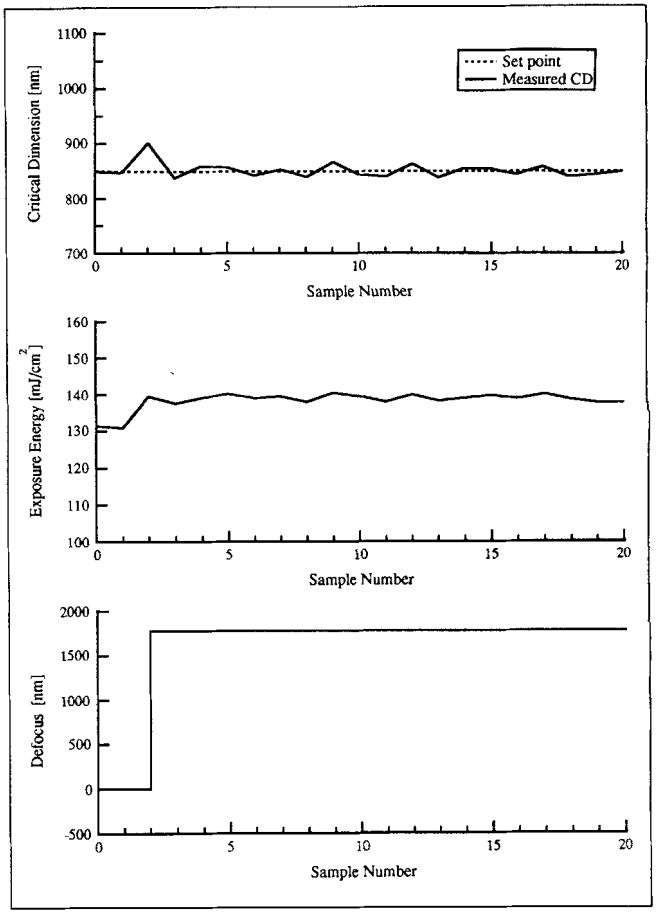

Figure 10. Defocus disturbance: closed-loop response of an adaptive NMIC controller with on-line parameter estimation.

the exposure energy to counter the effects of the defocus disturbance. The controller successfully brings the *CD* to the set point. In this simulation, a forgetting factor $\lambda = 0.5$ and a forgetting horizon $j^* = 50$ are used to discount old *CD* measurements. Figure 11 shows the evolution of the three estimated LPM parameters as functions of time. They are adjusted by the parameter estimator from their initial values (corresponding to the perfectly focused process) until they converge to a final state (corresponding to the defocused process).

Subjecting the NMIC controller to a defocus constitutes a particularly significant test. Note that the most natural way in which the Hershel-Mack model can account for defocus effects is by adjusting the intensity distribution function in Eq. 1a. However, in all the simulations presented here, the nature of the disturbance is assumed to be unknown; thus, the parameter estimation mechanism is constrained to find an adequate process model by adjusting only the three available model parameters, while leaving the intensity distribution function fixed at its nominal value. The NMIC controller performs well despite the fact that the model is prevented from exercising one of its degrees of freedom, namely, a true correction for defocus errors.

Absorptivity disturbance

Changes in the absorptivity of the resist material naturally occur due to thermal degradation, aging during prolonged storage, and inconsistencies in the supplier's stock quality. Figure 12 shows that an adaptive NMIC controller with on-line estimation is quite successful in rejecting the effect of a large change in the absorptivity of the resist photoactive component represented by a change in Dill's absorption parameter *A* (Dill et al., 1975). The evolution of the three estimated model parameters in Figure 13 is rapid, since they converge to new values shortly after the disturbance occurs. In this simulation, neither data filtering nor control deadband are used ($\alpha_e = \alpha_c = 0$ and $\Delta E_{\min} = 0$).

Effect of estimation filtering and control filtering on closed-loop performance

The estimation and control filters in Eqs. 4 and 7 are designed to attenuate the effects of measurement noise. To evaluate the effects of filtering on controller performance, a simulation is carried out in which the photolithography process experiences a defocus disturbance similar to that shown in Figure 10; however, in this case, the simulated *CD* measurements are deliberately corrupted by noise. The noise is assumed to be zero-mean Gaussian with a standard deviation of 10 nm.

The top part of Figure 14 compares (i) the open-loop *CD* response of the process, (ii) the closed-loop *CD* response using an on-line adaptive NMIC controller without data filtering

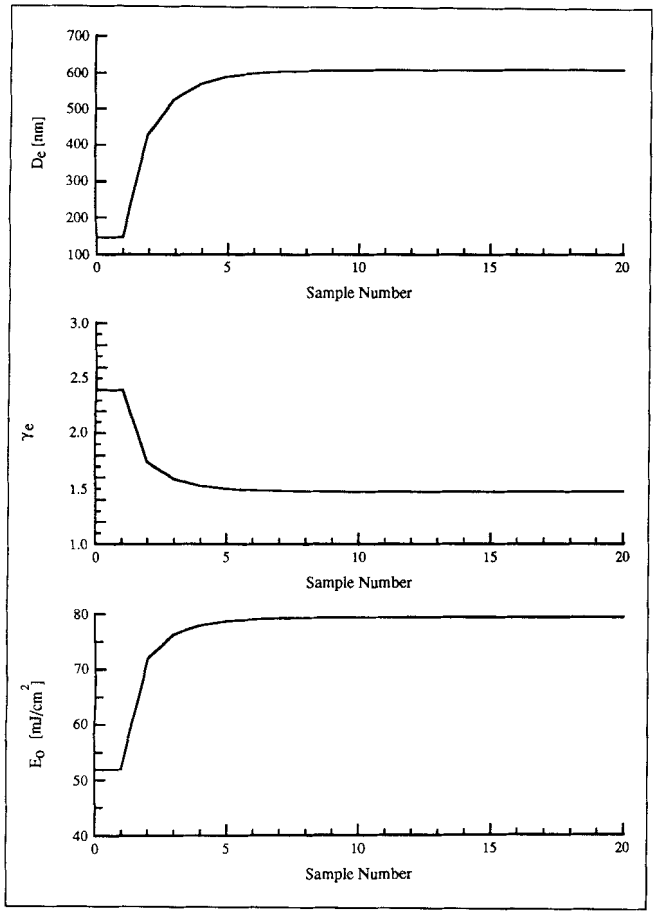

Figure 11. Evolution of estimated LPM parameters for the on-line adaptive controller of Figure 10.

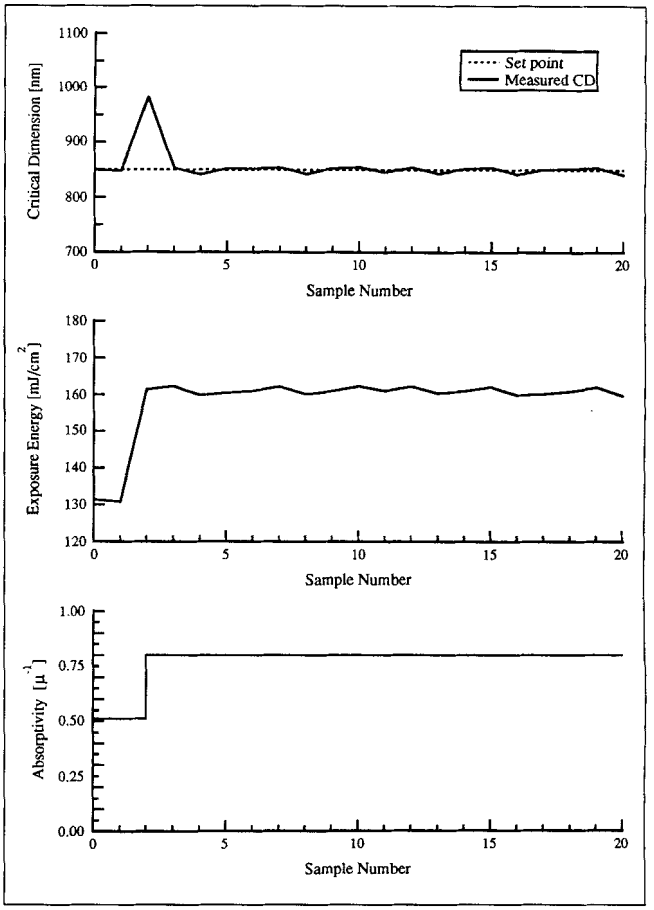

Figure 12. Absorptivity disturbance: closed-loop response of an NMIC controller with on-line parameter estimation.

($\alpha_e = \alpha_c = 0$), and (iii) the closed-loop *CD* response using an on-line adaptive NMIC controller with both estimation and control filtering ($\alpha_e = \alpha_c = 0.6$). Although the NMIC controller without data filtering succeeds in centering the *CD* about the set point, the exposure energy adjustments are abrupt and not smooth because the controller responds to noise-induced randomness in the measurements. A significant performance improvement is obtained using the estimation and control filters, as demonstrated by the smoother exposure energy adjustments curves. Figure 15 shows the favorable effects of the estimation filter on the estimated process parameters, which exhibit smooth changes.

Effect of control deadband on closed-loop performance

The NMIC controller can be constrained so that it avoids making exposure changes smaller than a user-specified deadband of width $2(\Delta E_{\min})$. The intention is to prevent the controller from making unnecessary exposure adjustments. Clearly, the deadband should be chosen to be at least equal to the energy delivered by the fastest shutter speed attainable with the stepper. Larger values can be chosen to allow only exposure energy adjustments that will bring about significant *CD* changes. On the other hand, inappropriately large values of $\Delta E_{\min}$ can effectively prevent the controller from making necessary process adjustments, resulting in an offset or steady-state error in *CD*.

The beneficial effects of using a controller deadband are illustrated in Figure 16, where the set-point changes of Figure 5 are repeated, except that now the effects of three deadband values are investigated: $\Delta E_{\min} = 0$, 0.3 mJ/cm^2 and 0.6 mJ/cm^2. The case of zero deadband is identical to that of Figure 5, where after the initial transient the CD trajectory displays occasional deviations from set point instead of settling to a single value. Figure 16 shows that by using a deadband of 0.3 mJ/cm^2, an excellent *CD* trajectory is obtained when the set point is reached. The excellent performance of the controller constrained by a 0.3 mJ/cm^2 deadband is not preserved for the 0.6 mJ/cm^2 deadband, which causes an undesirable *CD* offset. This result illustrates the adverse effect of a deadband that is chosen too large.

Conclusions

A model-based adaptive control technique for photolithography that is capable of delivering excellent performance has been developed and evaluated. The design consists of a reduced-order lithography model, an on-line parameter estimator, and a nonlinear model-inversion controller. The width

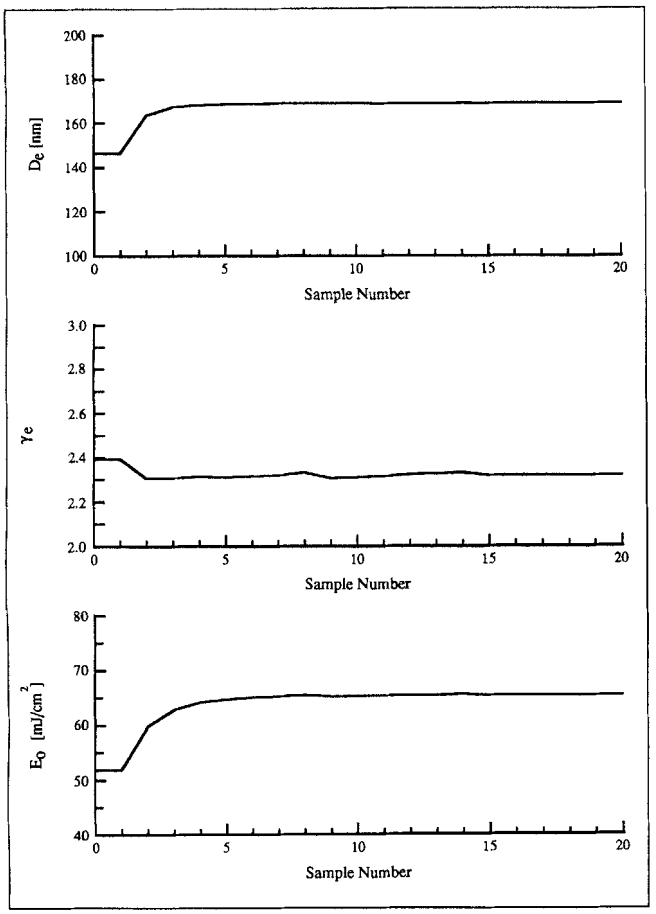

Figure 13. Evolution of the estimated LPM parameters for the on-line adaptive controller of Figure 12.

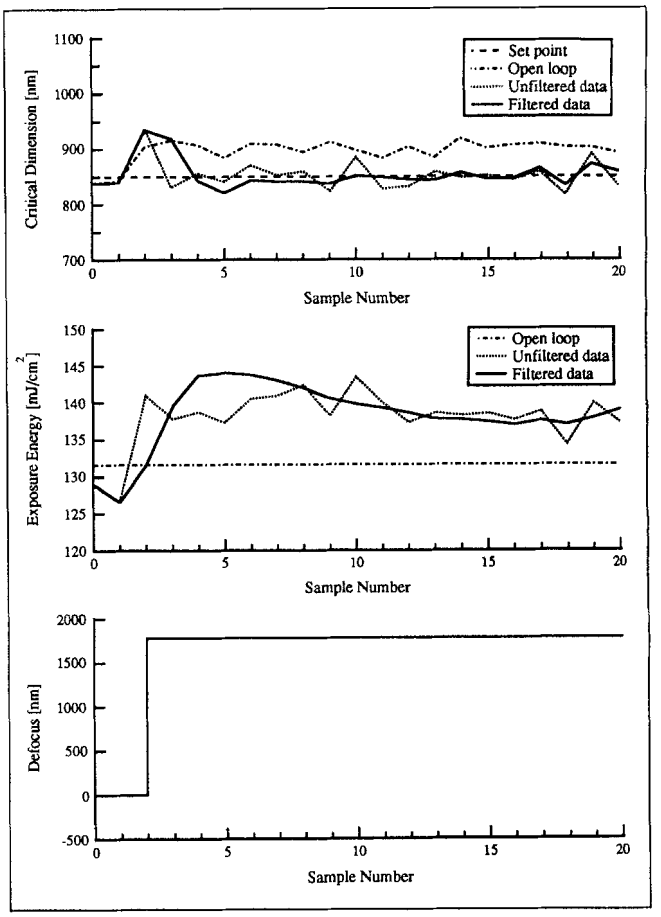

Figure 14. Defocus disturbance: response of adaptive NMIC controllers with on-line parameter estimation using estimation and control filters.

of the printed resist lines (the critical dimension) is controlled by automatically adjusting the exposure energy.

A series of simulated set-point changes demonstrated that a nonadaptive NMIC controller can track an arbitrary set-point trajectory. Good tracking performance is obtained even in the region where the model does not fit the process with great accuracy. This robustness against model errors is a valuable feature of the NMIC structure. An important advantage of the NMIC strategy is the capability of effectively rejecting the effect of unmeasured process disturbances on the critical dimension. Simulation studies show that a nonadaptive controller (the case where the LPM parameters remain fixed at all times) can neutralize the effects of certain types of disturbances, such as thickness changes. Other disturbances, however, change the process characteristics to the extent that adaptive control has to be used to realize the desired performance.

The cornerstone of the adaptive strategy is the capability of using process data to estimate on-line three photolithography model parameters: the effective photosensitivity, the effective contrast, and the effective thickness. Nonlinear regression techniques provide estimates of the model parameters using standard software. The adaptive NMIC design prevents the corruption of parameter estimates by incorporating provisions for forgetting past data and for attenuating measurement noise via filtering. A salient advantage of the proposed control strategy is that all the control activities are fully automated, thus significantly reducing the need for engineering intervention and contributing to the reduction of operating costs. In addition, no *ad hoc* controller tuning effort is involved. The parameter estimation technique is a least-squares optimization procedure that can be completely automated, again removing the need for engineering intervention in the modeling phase.

Closed-loop adaptive control of photolithography emerges from the analysis presented here as a powerful strategy that can successfully deliver excellent process performance. The adaptive NMIC technique is a specific realization of a model-based adaptive strategy and should be viewed as a valuable complement to other control strategies, such as SPC, in maximizing the effectiveness of an overall manufacturing control program. The strategy presented can be used as a paradigm for the development of adaptive control strategies for other processes used in the manufacture of microelectronic, photonic or micromechanical devices.

Acknowledgment

The simulation code used in this study is a modification of a lithography driver program originally written by Dave Hoerger and Steve Keifling. Critical dimension data were provided by the Intel

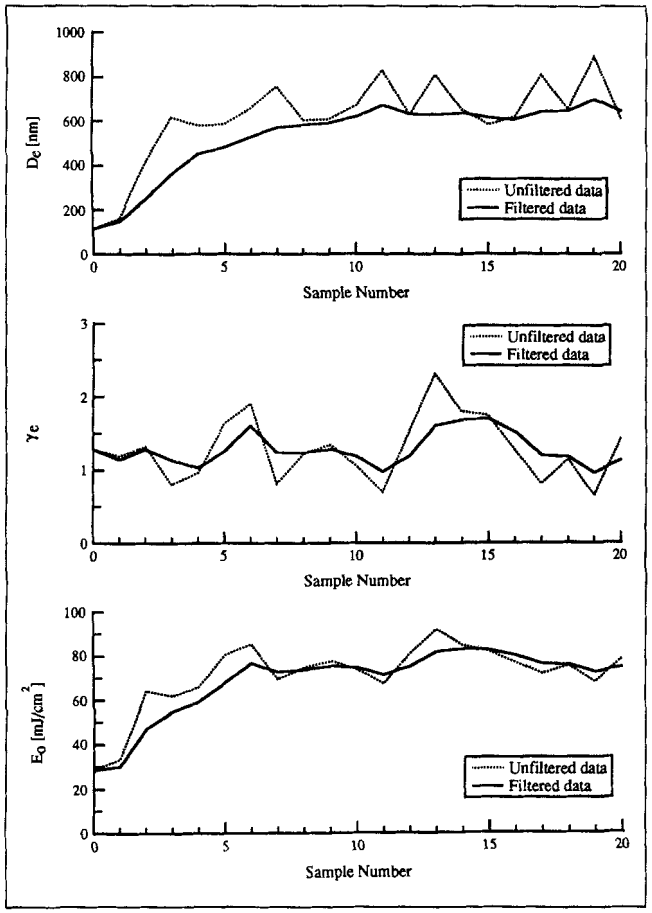

Figure 15. Evolution of estimated LPM parameters for the on-line adaptive controllers of Figure 14.

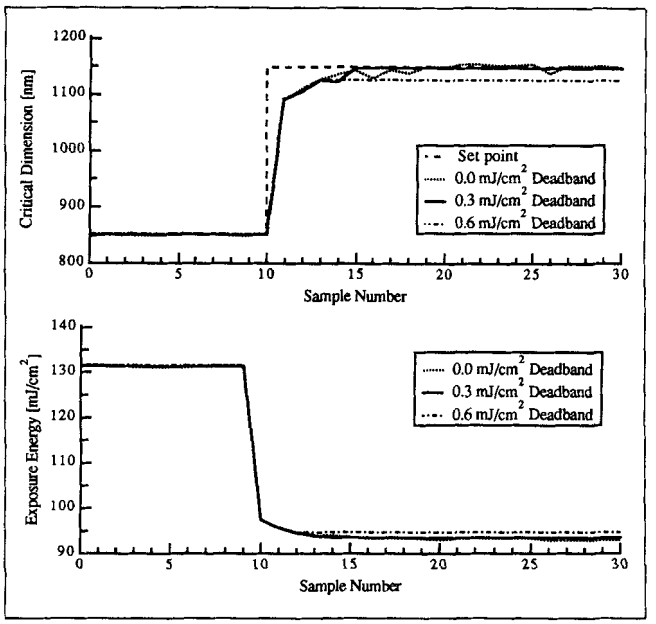

Figure 16. Effect of the control deadband on closed-loop performance.

Corporation. Support received from the Semiconductor Research Corporation under Contract No. 89-MJ-155 is gratefully acknowledged.

Notation

CD = critical dimension, nm
CD'' = filtered critical dimension measurement used for control, nm
CD_i = critical dimension measurement at location i, nm
CD_i' = filtered critical dimension measurement at location i, nm
$\widehat{CD}$ = estimated critical dimension, nm
$\widehat{CD}_i$ = estimated critical dimension at location i, nm
CD^s = critical dimension set point, nm
D' = actual resist thickness, nm
D_e = effective resist thickness, nm
E = exposure energy, mJ/cm^2
E_i = exposure energy applied to location i, mJ/cm^2
E_o' = actual photosensitivity, mJ/cm^2
E_o = effective photosensitivity, mJ/cm^2
$\Delta E_{\min}$ = control deadband, mJ/cm^2
i = measurement number
$I(\xi)$ = aerial intensity distribution, dimensionless
j^* = forgetting horizon
J = error function, nm^2
N = number of measurements used for parameter estimation
P = photomask pitch, nm
t = sample number

Greek letters

α_c = control filter constant, dimensionless
α_e = estimation filter constant, dimensionless
γ' = actual resist contrast, dimensionless
γ_e = effective resist contrast, dimensionless
ϵ_i = modelling error residual at location i, nm
λ = forgetting factor, dimensionless
ξ = horizontal location on mask, nm

Literature Cited

Bernard, D. A, "Optical Lithography Simulation: Introduction to SPESA," *Microelectr. Eng.*, **3**, 379 (1985).

Bruce, J. A., R. K. Leidy, M. S. Hibbs, and B. J. Lin, "Characterization and Prediction of Linewidth Variation due to Thin Film Interference Effects," *KTI Interface '88*, 301 (1989).

Chiu, W. K., and G. B. Wetherill, "A Simplified Scheme for the Economic Design of Charts," *J. of Quality Technol.*, **6**, 63 (1974).

Crisalle, O. D., S. R. Keifling, D. E. Seborg, and D. A. Mellichamp, "A Comparison of the SAMPLE and PROLITH Simulators for Optical Projection Lithography," *SPIE Microelectronic Integrated Processing—Growth, Monitoring, and Control*, **1185**, 171 (1989).

Crisalle, O. D., "Studies in Model-Based and Adaptive Control with Applications to Photolithography," PhD Thesis, Univ. of California, Santa Barbara (1990).

Dennis, J. E., and R. B. Schnabel, *Numerical Methods for Unconstrained Optimization and Nonlinear Equations*, Prentice-Hall, Englewood Cliffs, NJ (1983).

Diamond, W. J., *Practical Experiment Designs for Engineers and Scientists*, Van Nostrand Reinhold (1981).

Dill, F. H., W. P. Hornberger, P. S. Hauge, and J. M. Shaw, "Characterization of Positive Photoresist," *IEEE Trans. Electron. Dev.*, **ED-22**, 445 (1975).

Duncan, A. J., "The Economic Design of $\bar{X}$ Charts Used to Maintain Current Control of a Process," *J. Amer. Statistical Assoc.*, **51**, 228 (1956).

Duncan, A. J., "The Economic Design of $\bar{X}$ Charts When there is a Multiplicity of Assignable Causes," *J. Amer. Statistical Assoc.*, **66**, 107 (1971).

Economou, C. G., M. Morari, and B. Palsson, "Internal Model Control: 5. Extension to Nonlinear Systems," *Ind. Eng. Chem. Process Des. Dev.*, **25**, 403 (1986).

Edgar, T. F., and D. M. Himmelblau, *Optimization of Chemical Processes*, McGraw-Hill, New York (1988).

Fair, R. B., "Challenges to Manufacturing Submicron, Ultra-Large Scale Integrated Circuits," *Proc. IEEE*, **78**(11), 1687 (1990).
Garcia, C. E., and M. Morari, "Internal Model Control: 1. A Unifying Review and some New Results," *Ind. Eng. Chem. Process Des. Dev.*, **21**, 308 (1982).
Garza, C. M., and S. P. Grindle, "Resist Characterization and Optimization Using a Development Simulation Computer Program, PROSIM," *SPIE Advances in Resist Technology and Processing III*, **631**, 117 (1986).
Henson, M. A., and D. E. Seborg, "An Internal Model Control Strategy for Nonlinear Systems," *AIChE J.*, **37**, 1065 (1991).
Hershel, R., and C. A. Mack, "Lumped Parameter Model for Optical Lithography," Chap. 2, *Lithography for VLSI, VLSI Electronics—Microstructure Science*, R. K. Watts and N. G. Einspruch, eds., Academic Press, New York (1987).
Hoerger, D. L., "An Application of Artificial Intelligence Concepts to Supervisory Control of Photolithography," MS Thesis, Univ. of California, Santa Barbara (1988).
Hoerger, D. L., D. A. Mellichamp, and D. E. Seborg, "Supervisory Control for Semiconductor Processing," *Proc. Amer. Control Conf.*, **1**, 90, San Diego, CA (1990).
Jensen, K. F., "Control Problems in Microelectronics Processing," *Proc. Int. Conf. on Chem. Process Control (CPC III)*, M. Morari and T. J. McAvoy, eds., 623, Elsevier Science Publishers, New York (1986).
Lauchlan, L., K. Sautter, T. Batchelder, and J. Irwing, "In-line Automatic Photoresist Process Control," *SPIE Adv. in Photoresist Process. and Technol. II*, **539**, 227 (1985).
Levy, K., "Productivity and Process Feedback," *Solid State Technol.*, **27**(7), 103 (1984).
Ljung, L., *System Identification—Theory for the User*, Prentice-Hall, Englewood Cliffs, NJ (1987).
Lorenzen, T. J., and L. C. Vance, "The Economic Design of Control Charts: A Unified Approach," *Technometrics*, **28**(1), 3 (1986).
Mack, C. A., "PROLITH: A Comprehensive Optical Lithography Model," *SPIE Optical Microlithography IV*, **538**, 207 (1985).
Mack, C. A., A. Stephanakis, and R. Hershel, "Lumped Parameter Model of the Photolithographic Process," *Kodak Microelectronics Seminar, Interface '86*, San Diego, CA (1987).
Moré, J. J., B. S. Garbow, and K. E. Hillstrom, "User Guide for MINPACK-1," Argonne National Labs Report ANL-80-74 (1980).
Nagaswami, V. R., "Focus and Overlay Optimization for Submicron i-line Production Lithography," *KTI Interface '88*, 301 (1989).
Norton, A., and S. Cheng, "The Stepper Image Monitor: Sanity for the Wafer Stepper User," *Technical Proc. Semicon/West*, San Mateo, CA (1988).
Oldham, W. G., S. N. Nandgaonkar, A. R., Neureuther, and M. M. O'Toole, "A General Simulator for VLSI Lithography and Etching Processes. Part I—Application to Projection Lithography," *IEEE Trans. on Electron. Dev.*, **ED-26**, 717 (1979).
Ramirez, F. W., and T. A. Carroll, "On-Line State and Parameter Identification of Positive Photoresist Development," *AIChE J.*, **36**, 1046 (1990).
Seborg, D. E., T. F. Edgar, and S. L. Shah, "Adaptive Control Strategies for Process Control: A Survey," *AIChE J.*, **32**, 881 (1986).
Seborg, D. E., T. F. Edgar, and D. A. Mellichamp, *Process Dynamics and Control*, Wiley, New York (1989).
Shewhart, W. A., *Statistical Method from the Viewpoint of Quality Control*, Dover Publications, New York (1986).
Subramanian, S., "Rapid Calculation of Defocused Partially Coherent Images," *Appl. Optics*, **20**(10), 1854 (1981).
Thompson, L. F., C. G. Wilson, and M. J. Bowden, eds., *Introduction to Microlithography*, ACS Symp. Ser., **219**, Amer. Chem. Soc., Washington, DC (1983).
Yeung, M. S. "Modeling High Numerical Aperture Optical Lithography," *SPIE Optical/Laser Microlithography*, **922**, 149 (1988).
Youla, D. C., J. J. Bongiorno, and H. A Jabr, "Modern Wiener-Hopf Design of Optimal Controller: I. The Single-Input-Output Case," *IEEE Trans. Automatic Control*, **AC-21**, 3 (1976).

Manuscript received July 29, 1991.